Real-time infrared test set: assessment and characterization

H. Ronald Marlin, Richard Bates, Miles Sweet, and Rowena Carlson[a]
NCCOSC RDTE DIV D754,
San Diego, CA 92152-5000

R. Barry Johnson[b], Diehl H. Martin, Ronald Chung, Jon Geist
Optical E.T.C., Inc.,
3077-K Leeman Ferry Road, Huntsville, AL 35801

Michael Gaitan[c]
National Institute of Standards and Technology,
Gaithersburg, MD 20899

Charles Mulford, Eugene Zakar[d], and Robert J. Zeto
U.S. Army Research Laboratory,
AMSRL-PS-DA, Ft. Monmouth, NJ 07703

and

Russ Olson[e] and Gordon Perkins
The Titan Corporation,
3033 Science Park Road, San Diego, CA 92129

ABSTRACT

During the past several years, the technology for designing and fabricating thermal pixel arrays (TPAs) using silicon micromachined CMOS devices has been developed to support the development of a real-time infrared test set (RTIR) for sensors and seekers. The TPA is a custom application-specific integrated circuit device that is fabricated using a low-cost commercial CMOS process The RTIR is a compact, self-contained test instrument that is intended for test and evaluation of infrared systems in the field. This paper describes characterization of TPA pixels, including directional radiant intensity distribution, spatial radiance distribution, temperature distribution, cross talk, spectral radiance, air pressure effects, and rise and fall times.

Keywords: infrared projector, Hardware-In-The-Loop testing, infrared source, test set, infrared

---

Further author information-
[a] R.C.: E-Mail: rcarlson@nosc.mil; Telephone: 619-553-2505; FAX: 619-553-6842
[b] R.B.J.: E-Mail: oetc@iypn.com; Telephone: 205-880-8207; FAX: 205-880-3866
[c] M.G.: E-Mail: gaitan@nist.gov; Telephone: 301-975-2070; FAX: 301-948-4081
[d] E.Z.: Telephone: 908-427-2687; FAX: 908-427-2899
[e] R.O.: E-Mail: rolson@titan.com; Telephone: 619-552-9566; FAX: 619-552-9718

INTRODUCTION

The thermal pixel array (TPA) is a promising technology for low cost, rugged infrared scene simulation. It is made using a standard, commercial CMOS foundry process, with a subsequent maskless etch. Figure 1 shows a schematic view of one TPA pixel. A pixel is composed of a resistance-heated plate suspended over a pit. The pixel pitch, for the 64 by 64 array is 175 micrometers. The design of the resistor, and sizes of the hot plate and suspension struts may be varied to optimize temperature response and response time.

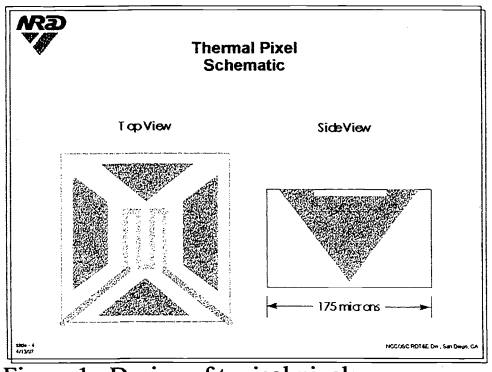

Figure 1. Design of typical pixel.

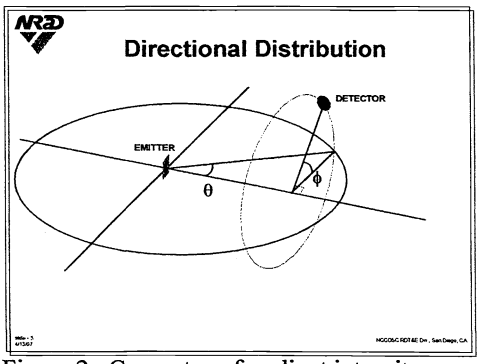

Figure 2. Geometry of radiant intensity directional distribution measurement.

A TPA array is formed by using standard CMOS techniques to lay down the circuitry on a silicon substrate. Driver circuits are formed on the periphery of the array, and bus lines to the resistive heaters are laid down along the pixel edges. An etch resistant glass mask, which defines the pixel and is open around the hot plate, is laid down as a final CMOS process step. A preferential etch for the silicon 1,1,1 planes is used to undercut the hot plate and struts to form a pyramidal pit underneath. The half-angle at the apex is approximately 57 degrees. This paper describes characterization of TPA pixels, including directional radiant intensity distribution, spatial radiance distribution, temperature distribution cross talk, spectral radiance, air pressure effects, and rise and fall times.

DIRECTIONAL RADIANT INTENSITY DISTRIBUTION

The directional radiant intensity distribution was measured under far field conditions by mounting the emitter in a two-axis goniometer and mounting a detector in a fixed position at a distance that is large compared with the dimensions of a pixel and normal to the surface of the emitter. Figure 2 shows the geometric relationships for the measurement. The angles of rotation are: theta, the rotation about an axis orthogonal to the emitter normal; and phi, the rotation about the normal. A data set consists of measurements taken at points with uniform angular spacing, over a hemisphere.

Because of the use of a large aperture (f/1.8) microscope objective (described below), it was important to determine that the directional distribution was uniform over a range of up to 21 degrees half angle.

The left plot in Figure 3 shows the relative radiant intensity distribution over theta, for values of phi from 0 to 360 degrees. The radial distance indicates the radiant intensity. A cosine function is shown for reference. Note that, for angles up to about twenty degrees from the normal (zero degrees), the radiant intensity is fairly constant and approximately lambertian; however, the distribution appears to be greater than lambertian at angles from about twenty to seventy degrees. This is probably due to radiation from the bottom of the hot plate reflected off the pit facets then passed through the spaces between the struts.

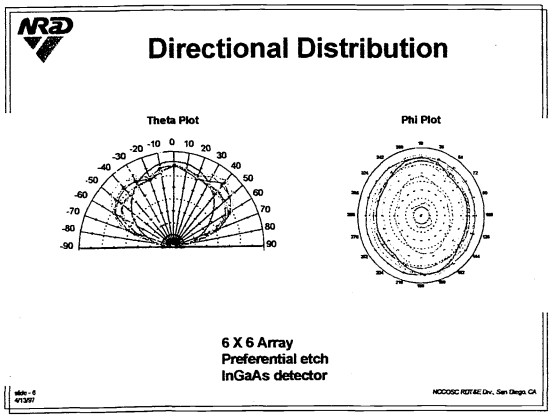

Figure 3. Directional distribution of radiant intensity.

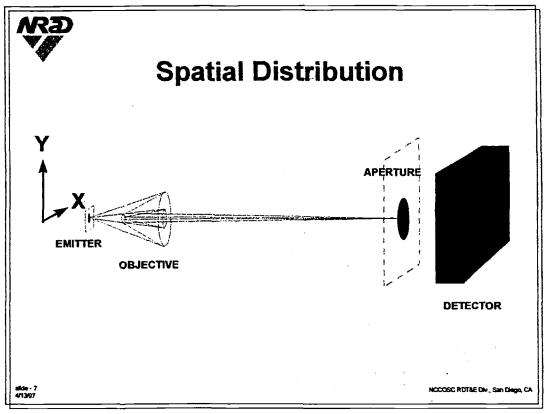

Figure 4. Spatial radiance distribution measurement.

The right plot in Figure 3 shows the relative radiant intensity distribution over phi for values of theta from 0 to 90 degrees. Radial distance indicates radiant intensity magnitude. Note that the distribution is generally circular; however, at very large values of theta (80 and 90 degrees indicated by the small, roughly rectangular shapes in the center) there appears to be two-fold symmetry in the data. This may be due to reflections off the edges of the hot plate. The one-fold symmetry data at higher theta values may indicate irregularities in some of the facet faces.

SPATIAL RADIANCE DISTRIBUTION

Figure 4 shows a schematic diagram of the micro-radiometer used to measure the distribution of radiance over the emitter surface. An Ealing 15X reflecting microscope images the emitter surface onto the image plane. A circular aperture at the image plane projected onto the emitter defines the radiant area seen by the detector. A 4 to 7 micrometer band-pass filter is inserted between the aperture and the detector. With the long wavelength limit of about 5.5 micrometers for the InSb detector, the band-pass of the system is about 4 to 5.5 micrometers. The diffraction limit of the objective at a wavelength of 5 micrometers is about 10 micrometers. An aperture of 200 micrometers gives a resolution of about 13 micrometers diameter at the pixel plane.

The emitter is mounted on an x-y translation stage. Data are obtained by translating the emitter in a raster pattern, moving the stage in increments, and pausing to take a datum at predetermined points. The operation is under computer control, and operating parameters, such as, scan rate, number of points, data averaging, etc., may be set by the operator. An optical chopper is inserted between the emitter and the objective. A computer controlled, lock-in amplifier is used to enhance the signal to noise ratio and sample averaging at each position may also be used.

The Ealing reflecting objective had a center obscuration, which allowed an entrance angular aperture of approximately eight to 21 degrees half angle; therefore, it was important to determine that the emitter had a uniform directional distribution within the acceptance angle.

TEMPERATURE CALIBRATION

The "electrical" temperature of NIST designed TPAs was determined by heating the chip on a hot plate and measuring the electrical resistance at various temperatures. A current-voltage (IV) curve was then run on several pixels (Figure 5). The relation between resistance and power was calculated, then the resistance was converted into temperature to give the graph shown in Figure 6.

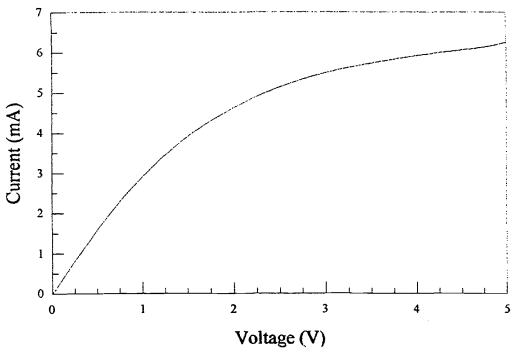

Figure 5. Current-voltage relationship for the OETC thermal pixel heater element with the chip maintained at ambient temperature.

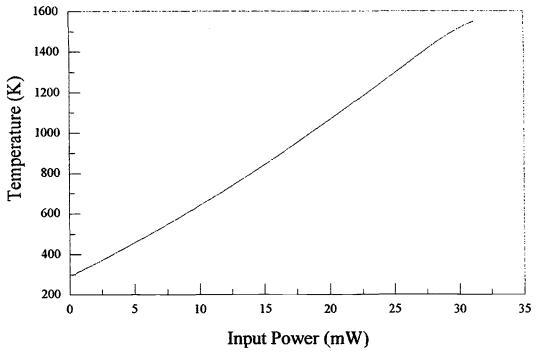

Figure 6. Electrical temperature versus input electrical power for the OETC thermal pixel heater element with the chip maintained at ambient temperature.

The micro-radiometer was calibrated to determine the relationship between the 4 to 5.5 micrometer band signal from a surface and its "effective" temperature (uncorrected for emissivity). The instrument with the 4 to 5.5 micrometer band pass filter was calibrated by positioning it to stare at the aperture of a blackbody. Signals were measured at various blackbody temperatures from 310 K to 500 K. Ignoring the emissivity a signal from a sample surface can be converted into an "effective" radiance and an "effective" temperature. Figure 7 shows the effective temperature calibration curve.

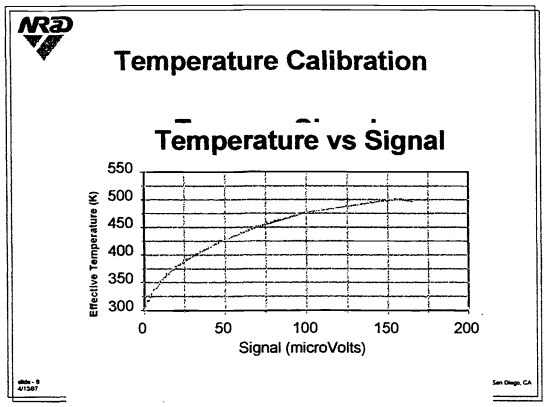

Figure 7. Temperature calibration of micro-radiometer

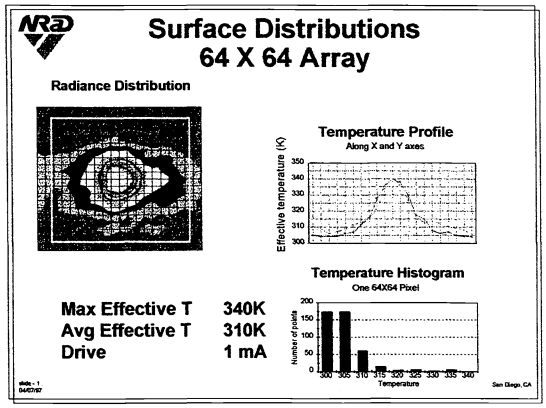

Figure 8. Surface distributions on one 64 by 64 pixel.

EFFECTIVE TEMPERATURE DISTRIBUTIONS

Figure 8 shows the effective temperature distribution over one pixel in an early 64 by 64 element array. A contour plot shows the two dimensional distribution of effective temperature. A white rectangle indicates the approximate pixel boundary. A profile plot shows the effective temperature along the x and y axes. A histogram shows the number of data points at different temperatures. An average effective temperature was calculated by summing the signals over the pixel area and dividing by the number of data points. This gave an average signal over the pixel, which is about seven percent of the peak. This was then converted into an average effective temperature, using the signal-to-temperature calibration curve. Similar plots for a larger scan covering one pixel and parts of its neighbors are shown in Figure 9. Again, a white rectangle indicates the approximate pixel boundary. Note that the profile plots show structure between the pixels. This is due to the bus lines running parallel to the pixel axes.

The 64 by 64 element arrays have on-board pixel drivers; the power to the pixels is determined by analog input currents. On the device tested, the input current was limited to about one milliampere. Small 2 by 3 element arrays, with the same hot plate design, but with direct electrical connections to the chip carrier pins, were measured to determine the input power-to-pixel temperature relationship. Figure 10 shows temperature distributions calculated from one dimensional scans across the center of the pixel. These arrays do not show structure at the edges of the pixels since they do not have bus lines.

CROSS TALK

The micro-radiometer was used to measure cross talk by powering one pixel and making a one dimensional scan of neighboring pixels. The experimental arrangement is shown in Figure 11. Because of the large dynamic range involved, the hot pixel was obscured to prevent its rays from entering the objective and scattering into the detector's field of view. A 400 micrometer wide absorbing baffle was formed from a chip of Red Spot velvet black paint, and glued to the arm of a micromanipulator. This black paint has a measured emissivity of 96 per cent in the 3 to 5 micrometers band. A highly absorptive material was necessary to minimize multiple reflections between its self and the device's surface. The diagram shows possible ray paths and shows that only the rays within the 8 to 21 degree half angle entrance aperture of the microscope objective would be likely to be detected.

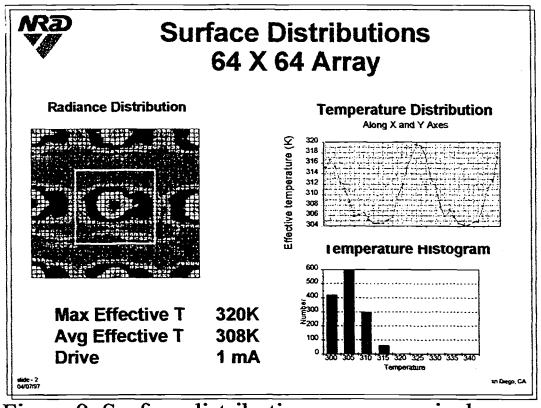

Figure 9. Surface distributions over one pixel and surroundings on 64 by 64 pixel.

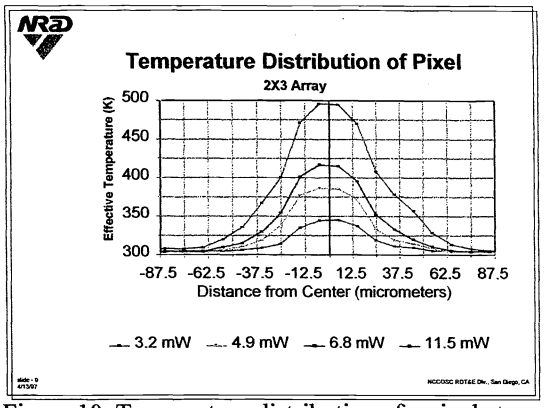

Figure 10. Temperature distribution of a pixel at several power levels.

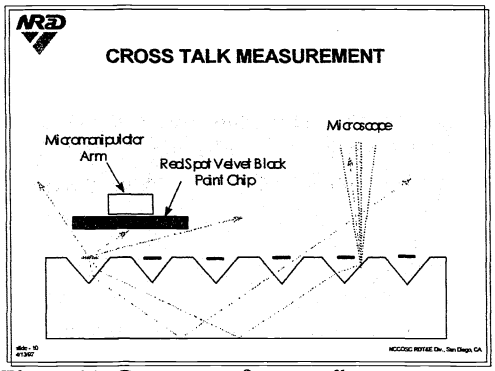

Figure 11. Geometry of cross talk measurement.

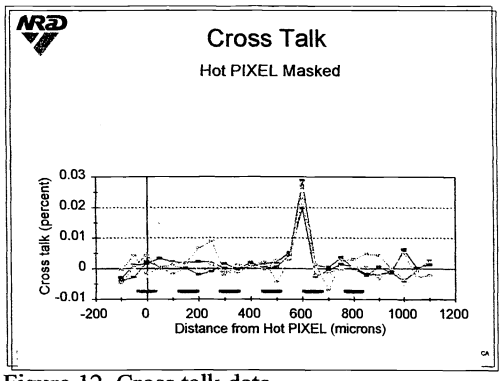

Figure 12. Cross talk data.

Figure 12 shows the results of scans made with the baffle placed at several heights above the hot pixel from about 10 and 100 micrometers. This was done for two reasons: first, it had previously been determined that objects close to a hot pixel in air could cool it significantly; second, because of the

possibility of rays reflecting between the baffle and the device surface, then into the objective. If the detected cross talk signal from the hot pixel increased with increasing baffle height, it would indicate that the temperature was changing; if the position of the apparent cross talk changed with baffle height, then the indication would be that there were reflections between the baffle and the device surface.

The data show a definite peak at one distance, for all baffle heights; and the height of the peak is fairly constant, within the noise limits. The cross talk appears to be approximately .025 per cent, about four or five pixels away from the hot pixel.

SPECTRAL RADIANCE

Spectral radiance measurements were made with a 250 millimeter, f/4, Ebert mount monochromator with a 75 lines per millimeter grating. The spectral resolution was about 0.1 micrometers. A 2.5 to 5 micrometer band-pass filter was used for order sorting. A spectral radiance standard with calibration to six micrometers, that is traceable to NIST was used to calibrate a ceramic heat lamp. This intermediate standard was used because of the wide dynamic range between signals from the standard lamp and the 64 by 64 array. Signals from the intermediate standard and the array were within the dynamic range of the experiment, so direct comparisons could be made with no changes in the setup.

The spectral radiance of an area of about 40 pixels (5 by 8) is plotted in Figure 13. Also plotted in the same figure, is the spectral radiance for a blackbody at the maximum temperature determined by the temperature distribution measurement and corrected for the effective radiance distribution.

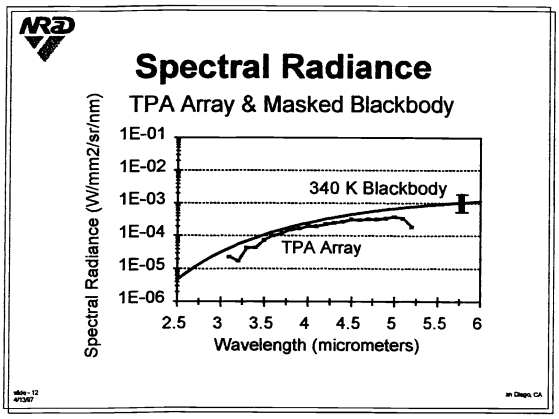

Figure 13. Spectral radiance of 64 by 64 array.

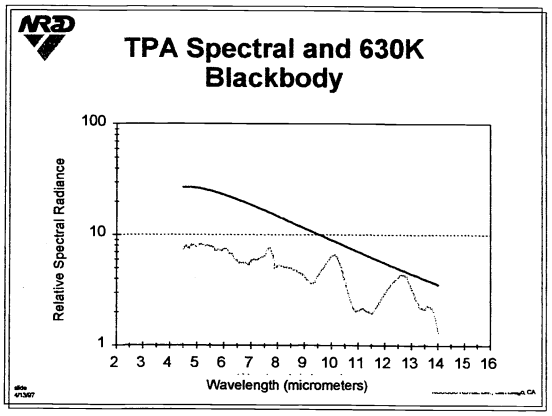

Figure 14. Relative spectral radiance of NIST designed pixel.

Figure 14 shows a plot of long wavelength relative spectral radiance from an NIST designed 6 by 6 element array. This measurement was made using the NRaD long wavelength spectral dewar. This device uses a cooled circular variable filter as a monochromator, with a liquid helium cooled, doped silicon detector. One pixel was imaged onto the entrance aperture. The relative spectral radiance of a 630 K blackbody is plotted for comparison. The long wavelength spectral radiance of current pixel designs has not been measured, but is scheduled for the near future.

PRESSURE EFFECTS

The pixel was driven with a square wave generator at ten hertz, and the output was adjusted to one milliampere at each pressure. The signal was measured with a lock-in amplifier. The effect of ambient pressure was measured by observing the radiation from one pixel in an array placed in an evacuable chamber. The array was placed close to a sapphire window in the end of the chamber. A liquid nitrogen cooled InSb detector in a sapphire windowed dewar was placed in proximity, so that the distance from pixel to detector was about 40 millimeters. The pressure variation from about .01 to 1.0 torr was

monitored with a thermocouple detector and from about 1.0 to 80 torr, with a mechanical gauge. The chamber was also opened to the atmosphere and a datum point was taken.

The fall off of signal with increasing pressure shown in Figure 15 suggests cooling of the hot pixel by ambient air. A plot of electrical resistance versus pressure (Figure 16) with the voltage and current data under the above conditions shows that the resistance is decreasing with increasing pressure. Since it was shown in Figure 5 that the resistance of the heater material increases with temperature, the cooling of the hot pixel by air is confirmed.

TEMPORAL CHARACTERIZATION

Rise and fall times for the 64 X 64 array were measured with the micro-radiometer, as shown in Figure 17. The pixels of a 4 by 64 section were addressed at a rate of approximately one MHz. A ten Hz square wave was applied to the analog input. The voltage across a 1000 ohm resistor measured the drive current. The data was stored on a digital oscilloscope and output to a pen plotter.

The oscilloscope output for the rise and fall time measurements is shown in Figure 18. The voltages across the resistor are shown with the signal from the detector. The 10 to 90 percent rise time is about 1.2 milliseconds. The fall time from 90 to 10 percent is about 0.9 milliseconds. These measurements were made at atmospheric pressure. Previous measurements on NIST designed arrays indicate about a 150 percent time increase in vacuum, so it is expected that the vacuum rise and fall times will be shorter than 2 milliseconds for the OETC designed arrays. Measurements of the relationship of temporal response and pressure for the 64 by 64 array are scheduled for the near future.

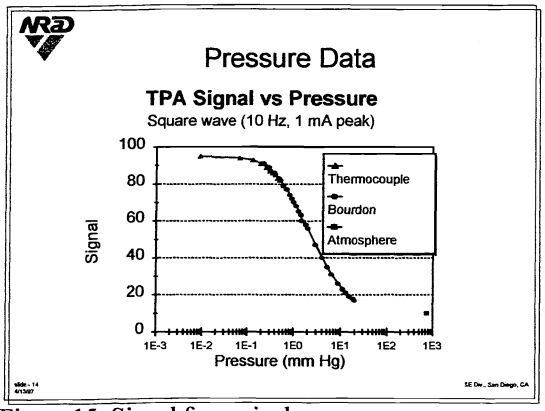

Figure 15. Signal from pixel versus pressure.

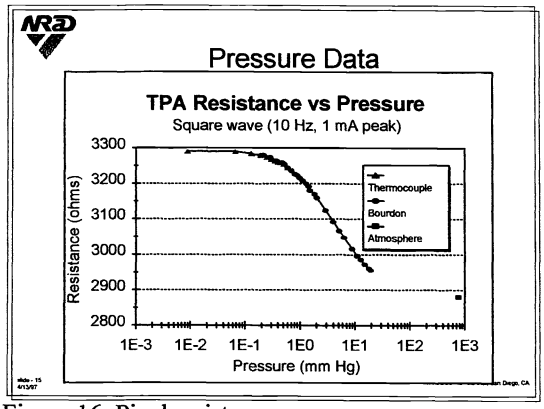

Figure 16. Pixel resistance versus pressure (constant current).

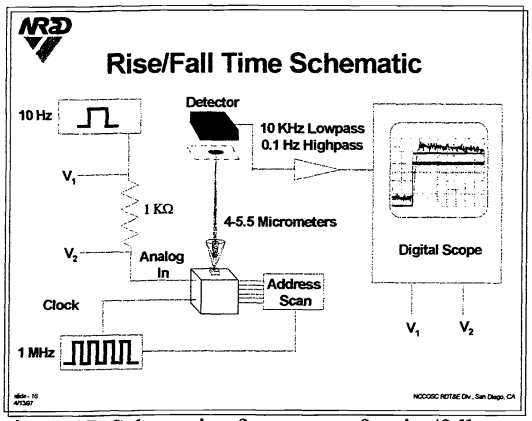

Figure 17. Schematic of apparatus for rise/fall time measurement.

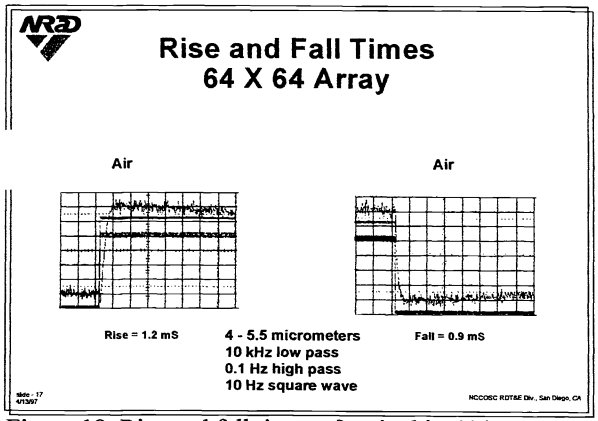

Figure 18. Rise and fall times of a pixel in 64 by 64 array.

CONCLUSION

Measurements were made, which included directional radiant intensity distribution, spatial radiance distribution, temperature distribution, cross talk, spectral radiance, air pressure effects, and rise and fall times. They indicate the viability for infrared scene simulation applications of micro-scale resistors and their arrays fabricated from a standard, commercial CMOS foundry process. These thermal pixel integrated circuits are a rugged and inexpensive outgrowth of the promising silicon micromachined resistive-array approach.

ACKNOWLEDGMENT

The RTIR program is funded by the Office of Naval Research LEAD Program, Dr. Phil Abraham, Code 331.

DISCLAIMER

DISCLOSURE NOTE

This technology may be the subject of one or more invention disclosures assignable to the U.S. Government. Licensing inquiries may be directed to:

Harvey Fendelman
Legal Counsel for Patents
NCCOSC, Code D0012
San Diego, CA 92152-5765
Telephone (619) 553-3001